MAUSAM, **72**, 1 (January 2021), 129-146

551.515.2 : 551.509.3

Tropical cyclone forecast using NCMRWF Global (12 km) and regional (4 km) models

RAGHAVENDRA ASHRIT, SUSHANT KUMAR, ANUMEHA DUBE, T. ARULALAN, S. KARUNASAGAR,

A. ROUTRAY, SAJI MOHANDAS, JOHN. P. GEORGE and A. K. MITRA

National Centre for Medium Range Weather Forecasting, Ministry of Earth Sciences,

A-50, Institutional Area, Phase-2, Sec-62, Noida (U.P.) – 201 309, India

e mail : raghu@ncmrwf.gov.in

सार – उत्तर हिंद महासागर (NIO) क्षेत्र के निकटवर्ती देश उष्णकटिबंधीय चक्रवातों (TCs) से विश्व के सर्वाधिक प्रभावित क्षेत्रों में से हैं। पिछले कुछ वर्षों में इस बेसिन को प्रभावित करने वाले उष्णकटिबंधीय चक्रवातों की आवृत्ति और तीव्रता में वृद्धि देखी गई है। उष्णकटिबंधीय चक्रवात की समय पर और सटीक भविष्यवाणी से इसके कारण होने वाली जन-धन की क्षति में कमी लाई जा सकती है। पिछले कुछसमय में, विभेदन,आँकड़ा समावेशन तकनीक में उन्नति तथासंख्यात्मक मौसम पूर्वानुमान (NWP) मॉडल की भौतिकी और मॉडल की प्रारंभिक स्थिति में सुधार के कारण उष्णकटिबंधीय चक्रवात के मार्ग तथा तीव्रता के पूर्वानुमानों मेंसुधार हुआ है। प्रस्तुत अध्ययन मेंहमने 16-21 मई, 2020 के दौरान बंगाल की खाड़ी के ऊपर आए महाचक्रवात (SuCS) 'अम्फन' के पूर्वानुमानों का विश्लेषण राष्ट्रीय मध्यम अवधि पूर्वानुमान केंद्र (NCMRWF) के यूनिफाइड मॉडल के वैश्विक और क्षेत्रीय संस्करण यानि NCUM-G और NCUM-R के माध्यम से से प्राप्त किया है। ट्रैक त्रुटि के विश्लेषण से पता चलता है कि दोनों मॉडलों में प्रारंभिक स्थिति और 24 घंटे के पूर्वानुमान की त्रुटियां बहुत समान हैं। हालांकि, NCUM-G की तुलना में NCUM-R में 48 से 72 घंटे की पूर्वानुमान त्रुटियां बहुत कम हैं। वैश्विक मॉडल से क्षेत्रीय मॉडल में ट्रैक त्रुटियों के प्रतिशत में कमी 48-घंटे के पूर्वानुमान में लगभग 12% और 72-घंटे के पूर्वानुमान में 17% है। NCUM-G में 18 मई, 2020 के बाद के पूर्वानुमानों में स्थल प्रवेश के स्थान की त्रुटि 50 कि.मी. से कम है। हालाँकि, स्थल प्रवेश के स्थान की त्रुटि NCUM-G की तुलना में NCUM-R में कम दिखाई देती है। NCUM-G और NCUM-R से तीव्रता के पूर्वानुमानों की तुलना से पता चलता है कि 16 मई, 2020 की प्रारंभिक स्थितियों के आधार पर न्यूनतम समुद्र स्तर के दबाव (SLP) के 48 घंटे के पूर्वानुमान प्रेक्षित तीव्रता के बहुत करीब हैं। 'अम्फन' की बहुत अधिक तीव्रता का भी, दोनों मॉडलों द्वारा अच्छी तरह से पूर्वानुमान (यद्यपि विलंब से) किया गया है। चक्रवात की संरचना से पता चलता है कि NCUM-G की तुलना में NCUM-R पूर्वानुमान में 850 hPa भ्रमिलताकोर अधिक सुदृढ़ है। NCUM-G पूर्वानुमानों की तुलना में NCUM-R पूर्वानुमानों में उष्ण-कोर प्रणाली भी अधिक व्यवस्थित है। दूसरी ओर, अधिकतम पवन की त्रिज्या NCUM-R की तुलना में NCUM-G पूर्वानुमान में अधिक होती है।

ABSTRACT. Countries adjoining the North Indian Ocean (NIO) region are among the world's worst affected areas by tropical cyclones (TCs). An increase in frequency and intensity of TCs affecting this basin is noticed in recent years. Timely and accurate prediction of a TC can lead to a decrease in damages to life and property caused by the cyclone. In recent times, the forecasts of TC tracks and intensity have improved due to advancements in the resolution, data assimilation techniques and physics of Numerical Weather Prediction (NWP) models and improvements in the model's initial condition. In this study, we have analysed the forecasts of Super Cyclone (SuCS) 'Amphan' that occurred over the Bay of Bengal during 16-21 May, 2020 obtained from the Global and Regional version of the NCMRWF Unified Model, *i.e.*, NCUM-G and NCUM-R, respectively.

The analysis of the track error shows that the initial position and 24-hour forecast errors in both the models are very close. However, the 48 to 72-hour forecast errors are much lower in the NCUM-R compared to NCUM-G. The percentage decrease in the track errors from global to regional model is about 12% in the 48-hour forecasts and 17% in the 72-hour forecasts. The landfall position error is less than 50 km in the predictions after 18th May, 2020 in NCUM-G. However, NCUM-R shows a lower landfall location error as compared to NCUM-G. Comparing the intensity forecasts from NCUM-G and NCUM-R shows that the 48 hrs forecast of minimum sea level pressure (SLP) based on initial conditions of 16th May, 2020 are very close to the observed intensity. The rapid intensification of Amphan is also well predicted by both the models, although with a delay. The cyclone structure shows that the 850 hPa vorticity core is much stronger in NCUM-R forecasts than NCUM-G. The warm-core system in the NCUM-R forecasts is also more organized than in NCUM-G. On the other hand, the maximum wind radius is greater in NCUM-G forecasts than NCUM-R.

Key words – Cyclone track errors, Landfall location error, Intensity verification, Rapid intensification, Regional models.

1. Introduction

The North Indian Ocean (NIO) is affected by tropical cyclones (TCs) in two seasons, namely, the pre-monsoon season, which lasts from March to May and the post-monsoon season which lasts from October to December (Mohanty *et al*., 2010). The intensity and frequency of cyclones have seen an increase over the NIO basin in recent years (Singh *et al*., 2000; Balaji *et al*., 2018). There were a total of 19 cyclones starting from 2018 to November 2020. Out of these cyclones, eight were intensified to the level of Severe Cyclonic Storms, 3 were Extremely Severe Cyclones and two were in the category of Super cyclonic storms. It can be seen that the number of intense cyclones is increasing in the NIO region and resulting in very significant damage to life and property. This damage can be minimized by a timely and accurate prediction of the cyclone's location and intensity.

In recent years, there has been a remarkable improvement in the forecasts of TCs using Numerical Weather Prediction (NWP) models. These improvements are due to the improvement in the resolution, data assimilation techniques as well as the physics of the NWP models (Mandal *et al*., 2003; Ashrit *et al*., 2006, Pattanayak *et al*., 2010; Osuri *et al*., 2013; Mohapatra *et al*., 2013; Routray *et al*., 2017a&b; Heming *et al*., 2019; Dutta *et al*., 2019). There have been several studies involving the global models for tropical cyclone forecasting. An exhaustive review is not attempted in this paper. TC analysis and forecast improvements demonstrated by assimilation of OSCAT surface winds in a global model (T574L64; Prasad *et al*., 2013) is one of the early demonstrations at NCMRWF using the global forecast model for TC. Usually, global NWP models, due to their coarser-resolution, cannot predict the intensity of the TC. Therefore a regional model with higher resolution and explicit convection is used. In an early study, Mandal *et al.* (2003) showed the improvement in the TC track forecasts over Bay of Bengal cyclones using a modified version of the regional model developed in collaboration with the Naval Research Laboratory (NRL) and North Carolina State University. Improved prediction of TC cases is due to increased resolution and assimilation of satellite data is also reported by Srinivas *et al*. (2010, 2012). Osuri *et al*. (2013), in their study, have compared the 18 and 9 km version of the Advanced Research version of Weather Research and Forecasting (ARW) model and show that the 9 km version has lower track errors with better intensity prediction. Impact of cyclone bogusing and data assimilation using WRF ARW (Chourasia *et al*., 2013), improved forecast of cyclone Phailin with 4DVAR assimilation (Iyengar *et al*., 2014), sensitivity to different convective parameterization schemes (Saji and Ashrit, 2014), the impact of assimilating Megha Tropiques SAPHIR radiances on tropical cyclone forecasts using WRF (Dhanya *et al*., 2016) are some of the important studies involving Bay of Bengal cyclones. Das *et al*. (2015) provides the first compilation of HWRF evaluation for North Indian Ocean tropical cyclones for all the cases during 2010-2013. The study based on nine TC cases showed an average track that displayed an improvement of 7, 27, 25 and 15% over the IMD operational forecasts at 36, 48, 60 and 72 h, respectively. The model with a high-resolution 3 km nest displayed a significant improvement in track forecasts with 12-46% over the model with a 9-km resolution nest. However, the HWRF model intensity forecasts showed only a marginal improvement of 5-8% over the IMD operational forecasts [Nadimpalli *et al*. (2020)]. Besides an improved intensity forecast, high-resolution regional models can predict the finer structure of a TC. The prediction of Bay of Bengal cyclones through assimilation of Doppler weather radar observations (Osuri *et al*., 2015) and prediction of rapid intensification (RI) using HWRF for the case of Phylin (Osuri *et al*., 2017) have improved. More recently using the Hurricane WRF (HWRF), Nadimpalli, *et al*. (2020) have demonstrated improved performance of HWRF against the quasi-operational WRF model forecasts of tropical cyclones over the Bay of Bengal. An evaluation carried out for 10 cases from 2013 to 2017 found a 27% improvement in skill over the quasi-operational WRF forecasts. The accurate prediction of TC's structure during landfall helps assess the distribution of strong winds and heavy rainfall, which can extend further inland, causing floods (Leroux *et al*., 2018). Several advances have been made in predicting a cyclone's structure in recent times (Heming and Goerss, 2010; Hazelton *et al*., 2018). Hazelton *et al*. (2018) have used a nested version of the finite-volume dynamical core (FV3) with GFS physics (fvGFS) to show that this model has the capability of predicting TC intensity and structure more accurately.

Super Cyclonic Storm (SuCS) Amphan was the first cyclone for the pre-monsoon cyclone season of 2020. It caused widespread damage over India's eastern part (particularly West Bengal, where it made landfall) during the period. As per the preliminary estimates (reported in media; CNN), total damage was estimated to be around 13.7 Billion USD. However, due to the Government of India's timely preparations, the loss of life was limited to 86. According to the India Meteorological Department (IMD), this was the strongest TC to occur in the BOB since the 1999 Odisha SuCS. Coastal areas of Odisha, particularly Paradeep, received extremely heavy rainfall amounts (>200 mm) of 24 hrs accumulated rainfall during 19-20 May, 2020 (IMD tropical cyclone bulletin of 20th May, 2020).

In this study, we have analysed the performance of the National Centre for Medium Range Weather

TABLE 1

NCMRWF Unified Model configuration since June 2018

Model	Application & domain	Resolution	Forecasts
NCUM-G	Global Deterministic Model	N1024L70 (12 km horizontal resolution with 70 vertical levels)	0000 UTC : Day 1 to Day 10 1200 UTC : Day 1 to Day 10
NCUM-R	Regional Deterministic Model high resolution over Indian region (5-40° N and 65-100° E)	4 km resolution Explicit convection	0000 UTC : Day 1 to Day 3 1200 UTC : Day 1 to Day 3

TABLE 2

Observations Assimilated in NCUM Global Data assimilation system

Observation type	Observation description	Assimilated Variables
AHIClear	Advanced Himawari Imager radiances from Himawari-8	Brightness Temperature (T_b)
Aircraft	Upper-air wind and temperature from aircraft	u, v, T
AIRS	Atmospheric Infrared Sounder onboard AQUA Satellite	T_b
AMSR	Radiances from AMSR-2 onboard GCOM satellite	T_b
ATOVS	AMSU-A (all sky), AMSU-B/MHS, HIRS from NOAA-18 &19, MetOp-A&B	T_b
ATMS	Advanced Technology Microwave Sounder in NPP satellite	T_b
CrIS	Cross-track Infrared Sensor observations in NPP satellite	T_b
FY3C	Radiances from Micro Wave Humidity Sounder (MWHS) of FY3C Satellite	T_b
GMI	Observations from Global Precipitation Measurement (GPM) Microwave Imager (GMI) instrument	T_b
GOESClear	Cloud clear Imager radiances from GOES	T_b
GPSRO	Global Positioning System Radio Occultation observations from various satellites (including MT-ROSA)	Bending Angle
Ground GPS	Ground based GPS observations from various locations	Zenith Total Delay
IASI	Infrared Atmospheric Sounding Interferometer from MetOp-A&B	T_b
INSAT-3D Sounder	INSAT-3D Sounder radiances	T_b
INSAT-3D Imager	Cloud clear Imager radiances from INSAT-3D	T_b
SAPHIR	SAPHIR microwave radiances from Megha-Tropiques	T_b
Satwind	Atmospheric Motion Vectors from various geostationary and polar orbiting satellites (including INSAT-3D)	u, v
Scatwind	Scattrometer observations (Ocean Surface Wind) from MetOp-A & B, ScatSat-1, WindSat	u, v
SEVIRIClear	Cloud clear observations from SEVIRI of METEOSAT 8 & METEOSAT 11	T_b
Sonde	Radiosonde observations, upper-air wind profile from pilot balloons, wind profiles, VAD wind observation from Indian DWR	u, v, T, q
Surface	Surface observations from Land and Ocean	u, v, T, q, P_s
SSMIS	SSMIS Radiances from DMSP satellites	T_b

TABLE 3

Salient features of NCUM assimilation - Forecast system

NCUM assimilation - Forecast system		
Model	Atmospheric Data Assimilation	Surface Analysis
Model: Unified Model; Version 10.8 **Domain:** Global **Resolution:** 12 km, Levels 70 **No. of Grids:** 2048 × 1536 **Time Step:** 5 minutes **Physical Parameterizations:** based on GA6.1 (Walters *et al*., 2017) **Dynamical Core:** ENDGame **Forecast length:** 10 days (based on 0000 UTC and 1200 UTC initial conditions)	**Resolution:** N320L70 (~40 km) with N144L70 Hessian based pre-conditioning **Method:** Hybrid incremental 4D-Var. Information on “errors of the day” is provided by NEPS forecast at every data assimilation cycle **Data Assimilation Cycles:** 4 analyses per day at 0000, 0600, 1200 and 1800 UTC. Observations within +/- 3 hrs from the cycle time is assimilated in respective DA cycle **Observations:** Observation Processing System does the quality control of observations. Variational bias correction is applied to satellite radiance observations	**Soil Moisture Analysis:** *Method:* Extended Kalman Filter *Analysis time:* 0000, 0600, 1200 and 1800 UTC *Observations assimilated:* ASCAT soil wetness observations, Screen level Temperature and Humidity (pseudo observations from 3D-Var screen analysis) **Sea Surface Temperature and Sea Ice:** Updated at 1200 UTC DA cycle with OSTIA based SST and sea-ice analysis **Snow Analysis:** Satellite-derived snow analysis. Updated at 1200 UTC DA cycle

Forecasting (NCMRWF) deterministic models in forecasting the Super Cyclone (SuCS) Amphan, which was observed during 16-21 May, 2020 over the Bay of Bengal (BOB). This study compares the forecast of increased grid resolution in the NCMRWF high resolution (4 km) regional model (NCUM-R) and (12 km) global model (NCUM-G). Both the models are being operationally used at NCMRWF for the numerical prediction of severe weather events over India. The NCMRWF Unified Model (NCUM) has been adapted from the Unified Model (UM) of the "UM Partnership). More details about the NCUM modeling system are given in the next sub-sections.

1.1. *NCMRWF Unified Modelling system*

The NCUM-G (Rajagopal *et al*., 2012; George *et al*., 2016) uses a seamless modeling approach, has a horizontal grid resolution of ~12 km and 70 vertical levels (reaching 80 km height), is being used for the 240 hrs numerical weather forecast since 2018 (Kumar *et al*., 2018a). This model and assimilation system have been updated periodically to adapt to various scientific and technical developments. Advanced END Game dynamical core is used in the model, which provides improved accuracy of the solution of primitive model equations and reduced damping. END Game also increases variability in the tropics, which leads to an improved representation of TCs and other tropical phenomena (Walters *et al*., 2017). An advanced data assimilation method Hybrid 4D-Var is used for the creation of NCUM global atmospheric analysis. Ensemble Transform Kalman Filter (ETKF) based on the NCUM ensemble prediction system (NEPS) provides flow-dependent background errors to this Hybrid 4D-Var system. Utmost importance has been given to the assimilation of Indian satellite observations in this data assimilation system. INSAT-3D Atmospheric Motion Vector (AMV), Megha Tropiques (MT)-SAPHIR radiance, Scatsat Ocean Surface Winds are being assimilated in the operational NCUM global data assimilation system, in addition to other global observations. A list of observations assimilated in the latest NCUM global data assimilation system is given in Table 2. Salient Features of NCUM Assimilation - Forecast System is shown in Table 3.

NCUM global data assimilation system produces analyses at 0000, 0600, 1200 and 1800 UTC. In each 6 hourly data assimilation cycle, the available observations distributed over the 6 hour assimilation window (center of the analysis cycle ± 3 hr) are combined with the model background to produce the NCUM-G analysis. Table 1 summarizes the model configurations operational at NCMRWF. Details on the model parameterization schemes, data assimilation, etc., can be found in Kumar *et al*. (2018b).

NCUM-R has a horizontal grid resolution of ~4 km and 80 vertical levels, with the model top at 38.5 km and 14 model levels below 1 km. The model has a time step of 1 minute. The model domain covers India and the adjacent oceanic regions and is operationally producing 72 hrs forecasts. In this convection-permitting model configuration, sub-grid scale deep convection is not parameterized. The prognostic cloud fraction and prognostic condensate (PC2) scheme used in this model is based on Wilson (2008a&b). The sub-grid turbulence scheme used is a blended scheme (Boutle *et al*., 2014), which dynamically combines the one-dimensional (1D) boundary-layer scheme of Lock *et al*. (2000) with a 3D

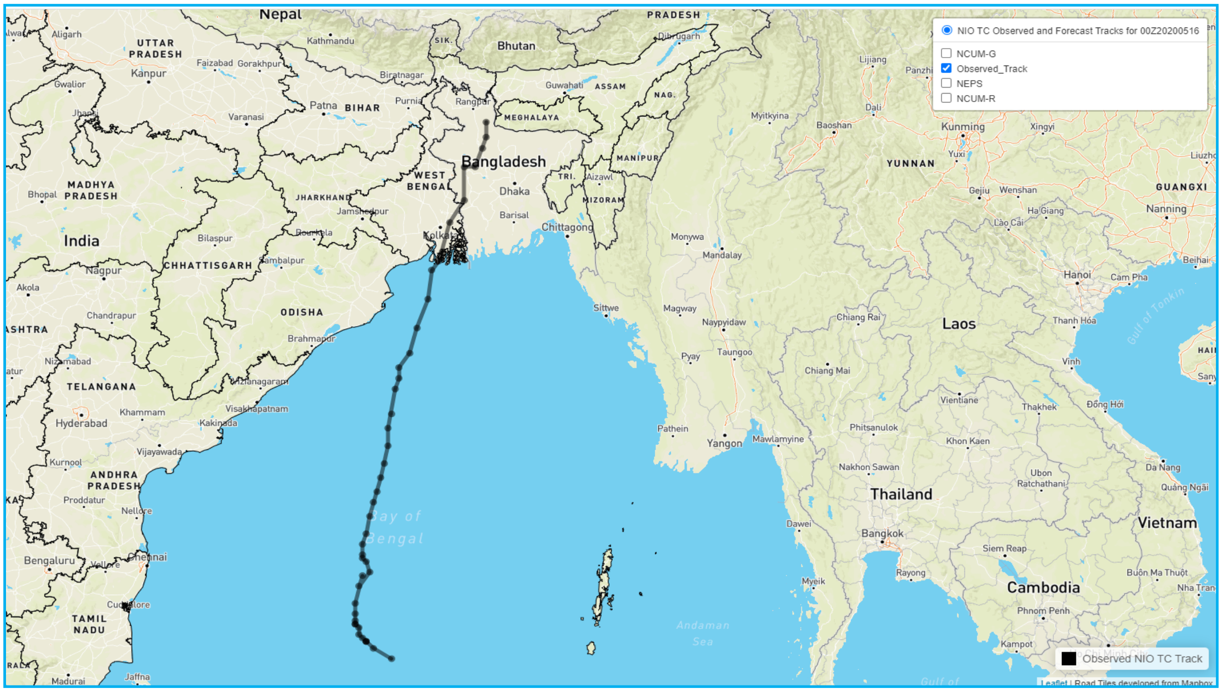

Fig. 1. Observed track of the Bay of Bengal Super Cyclone 'Amphan' during 15-21 May, 2020

Smagorinsky scheme using a mixing factor of 0.5. The model employs NASA Shuttle Radar Topographic Mission (SRTM) 90 m digital elevation map orography.

NCUM-R uses the high resolution analysis prepared by the 4D-Var data assimilation (DA) system. In addition to most of the observations used in the NCUM global data assimilation system (even though data thinning strategies are different), Indian Doppler Weather Radar observations of radial wind are also used in the regional DA system with a time window of ± 3hours. The model domain covers the South Asian region, covering BOB and part of the Arabian Sea (6° S -41° N and 62-106° E). The details of NCUM-R model configuration can be found in Dutta *et al.*, 2019; Jayakumar *et al.*, 2019 and Bush *et al.*, 2020.

1.2. *Variational data assimilation*

Data assimilation based on the 4D-Var method has been used to prepare an analysis (initial condition) for NCUM since 2012. A detailed description of the 4D-Var system can be seen in Rawlins *et al.* (2007); Rajagopal *et al.* (2012); John *et al.* (2016) and Kumar *et al.* (2018b). The 4D-Var system produces the analysis by minimizing a cost function (penalty function), which describes the departure of the analysis from background and observations. The 4D-Var uses the information of "background" or "first guess" (a short forecast from previous analysis), observations, as well as error statistics of background and observations. A drawback of 4D-Var is that the background error used in the system does not account for the day-to-day varying model errors due to the changes in the weather conditions. One way to include the everyday varying forecast error is by using ensemble forecasts to calculate the forecast uncertainty. So in 2016, the data assimilation system was upgraded to Hybrid 4D-Var (Kumar *et al.*, 2018a). The Hybrid 4D-Var system's advantage is that it uses "varying day-to-day flow-dependent" background errors in addition to "climatological" background errors. The Ensemble transformer Kalman Filter (ETKF) based ensemble prediction system at NCMRWF provides flow-dependent background errors to the Hybrid 4D-Var system. After that, improvements have been made in the data assimilation system to assimilate newer observations available with the global observing system. Utmost importance has been given to the assimilation of Indian satellite observations. Indian satellite observations of INSAT-3D imager and sounder radiance, INSAT-3D Atmospheric Motion Vector (AMV), Megha Tropiques (MT)-SAPHIR radiance, MT-ROSA Radio Occultation (RO), Scatsat Ocean Surface Winds are being assimilated in the latest operational NCUM Hybrid 4D-Var global data assimilation system. A list of observations assimilated in the latest NCUM global data assimilation system is given in Table 2. Salient features of NCUM-G Assimilation - Forecast System is provided in Table 3.

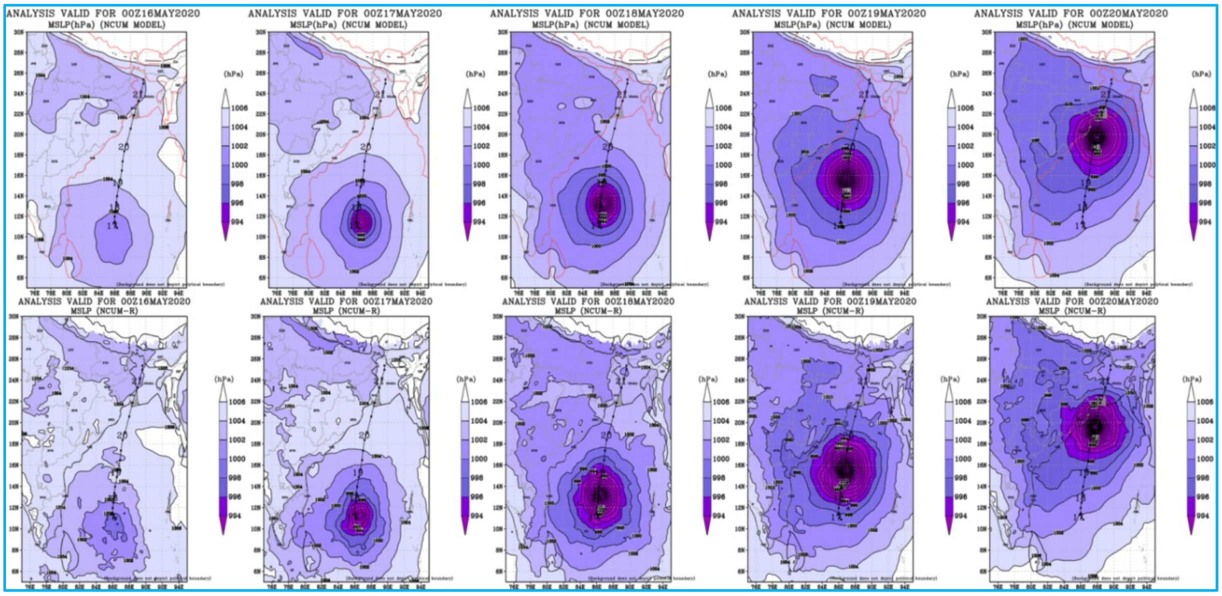

Fig. 2. The model analysis Mean Sea level Pressure (MSLP) in hPa over Bay of Bengal during 16-20 May, 2020 in the global model NCUM-G (top) and regional model NCUM-R (bottom). Observed track of the cyclone is also shown

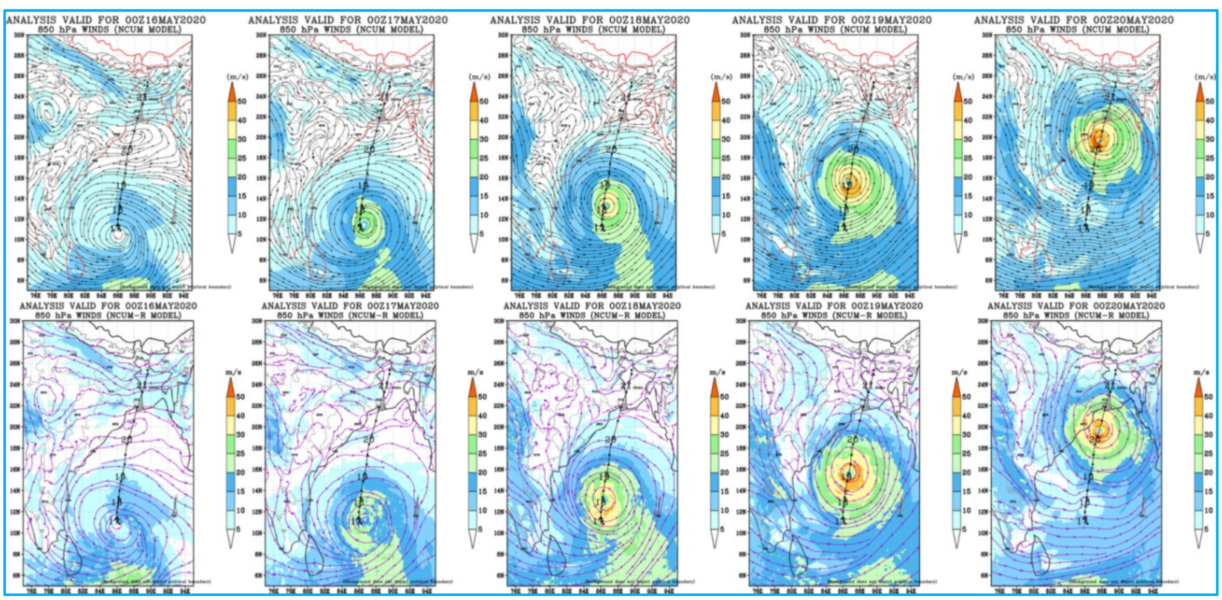

Fig. 3. The model analysis 850 hPa winds over Bay of Bengal during 16-20 May, 2020 in the global model NCUM-G (top) and regional model NCUM-R (bottom). Observed track of the cyclone is also shown

2. NCUM Global and regional analysis

The space-time evolution of Amphan cyclone in NCUM global and regional analysis is shown in Figs. 2&3 *via* the mean sea level pressure (MSLP) and 850 hPa winds. Observed cyclone track (solid black line) is also indicated in each panel to compare cyclone position in the model analysis. The performance of NCUM-G analysis and forecasts during the cyclone is discussed in terms of MSLP and 850 hPa level winds. It can be seen that global and regional analyses represented the system from the stage of a well-marked low-pressure system and its intensifications are reasonably well represented during the life-span of the cyclonic storm. During 16-17 May, 2020, within 12 hours or less, the system became more distinct as it gradually intensified into a depression,

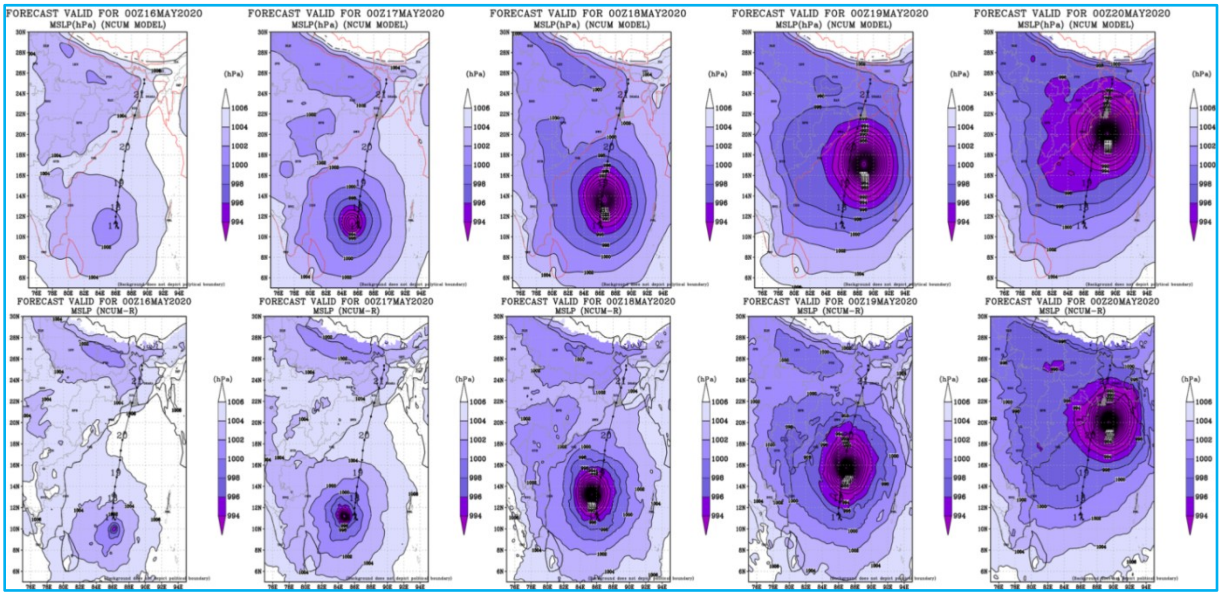

Fig. 4. The model forecast (Day-1) Mean Sea level Pressure (MSLP) in hPa over Bay of Bengal during 16-20 May, 2020 in the global model NCUM-G (top) and regional model NCUM-R (bottom). Observed track of the cyclone is also shown

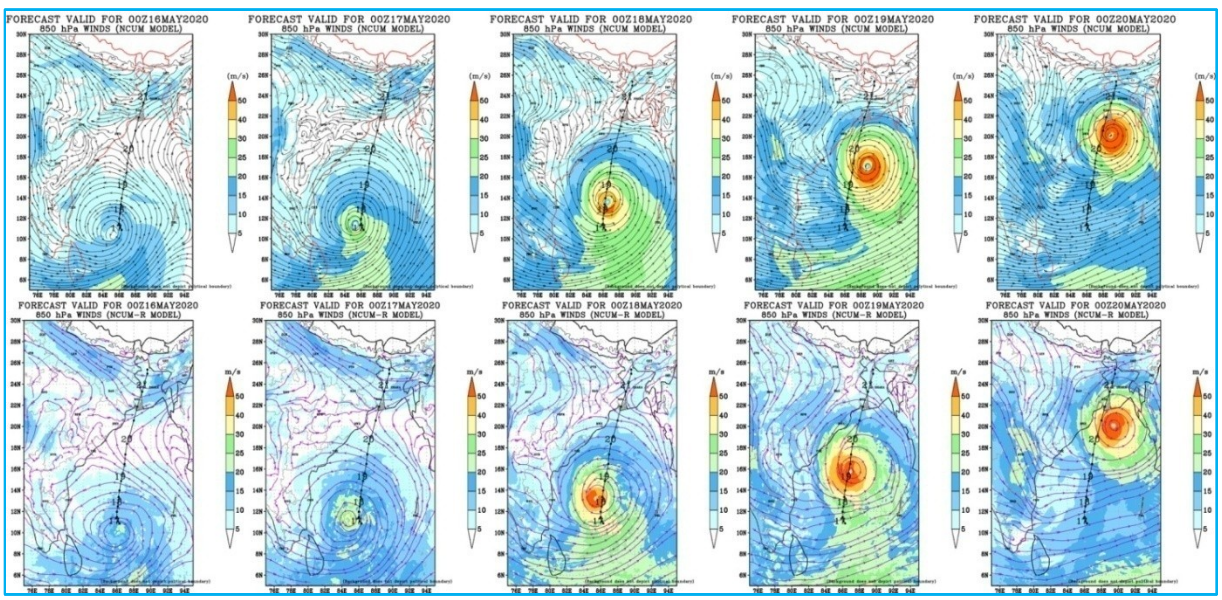

Fig. 5. The model forecast (Day-1) 850 hPa winds over Bay of Bengal during 16-20 May, 2020 in the global model NCUM-G (top) and regional model NCUM-R (bottom). Observed track of the cyclone is also shown

gaining from a prolonged stay over warm oceans. The system has spiral bands of deep convective clouds surrounding the system's low-pressure center, as evidenced by the streamlines (Fig. 3). Despite having a different resolution, the cyclone's intensity in analysis, in terms of wind speed in both global (Fig. 3; top) and regional (Fig. 3; bottom), agree well. Enhanced circular isobars and wind speeds in both global and regional analysis indicate the storm's intensification on 17^{th} May, 2020. A close correspondence in the movement and landfall also can be noticed from both the analysis.

3. NCUM Global and regional forecasts

In this section, a brief description of global and regional forecasts of the Amphan cyclone is discussed. When compared with the global analysis, the 24 hr (Day-1) forecast of MSLP and 850 hPa

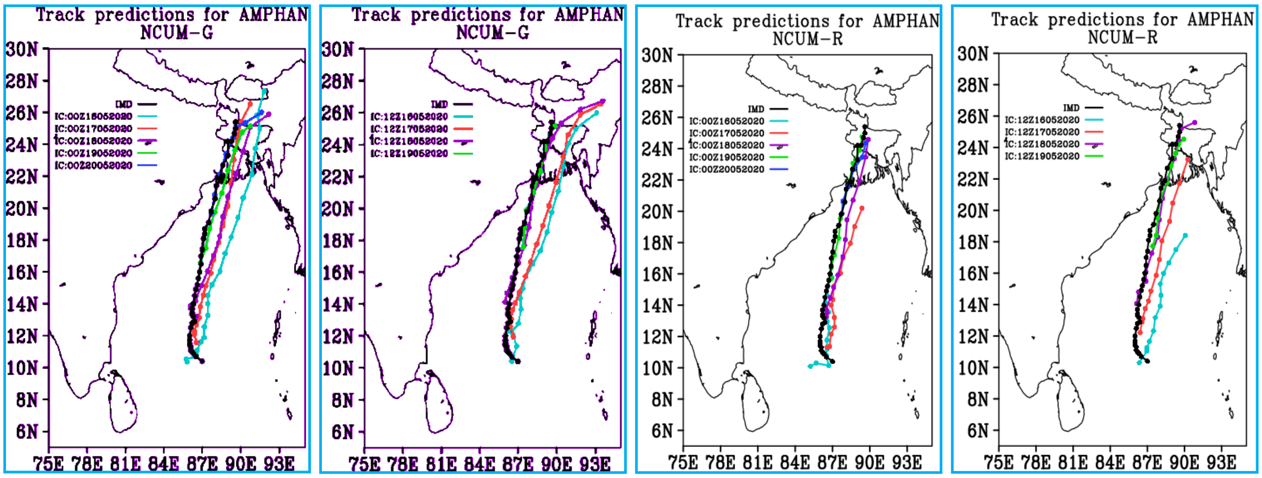

Fig. 6. Observed and model forecast tracks for cyclone Amphan based on NCUM-G (top) and NCUM-R (bottom) are shown for 0000 UTC (left) and 1200 UTC (right) forecasts during 16-20 May, 2020

winds (Fig. 4&5 respectively) show well-marked depression on 16th May, 2020, rapid intensification of the storm on 17th May, 2020, steady movement on the next couple of days and landfall on 20th May, 2020 agree well. As seen from the 850 hPa low-level winds, the intensity of the cyclone is also well predicted in global model forecasts (Fig. 5). Day-1 global NCUM forecasts on 18th May, 2020 show the system's North-west ward movement and landfall occurrence on the 20th May, 2020. Subsequently, Day-3 forecasts show the system has made a further inward movement towards land and located over west Bengal (not shown). As it moved further inland, it rapidly weakened. The storm was downgraded into Category 1, equivalent to Cyclonic Storm (CS), just six hours after landfall and became disorganized. On the other hand, the regional NCUM forecasts slightly overestimate the intensity at all the forecast times.

Further, in the regional NCUM, the center of the cyclone is slightly located south-eastward compared to the respective analysis and the IMD best track position (solid black line). This intensity overestimation in the regional NCUM Day-1 forecast is also evident in the winds (Fig. 5). It is interesting to note that the cyclone movement meanders in the regional model forecast compared to the best track with the lead time. For example, the cyclone center is situated on the westward side of the best track position during the rapid intensification period (on 17th May, 2020). In contrast, it moved to the east side of the track in the subsequent days.

4. Cyclone forecasts and its verification

The verification of cyclone forecasts involved evaluating the forecast tracks and intensity against the best track (BT) estimated. Additionally, verification of landfall position and time is also presented in this section based on the reported landfall position and time. Verification of Rapid Intensification (RI) of the SuSC Amphan is also assessed in the forecasts using the 24-hour change in the predicted wind speed by the models.

4.1. *The bi-variate TC Tracker*

The UK Met Office bi-variate approach to tracking TCs is used to track the location of the Super Cyclone ‘Amphan’. The bi-variate method identifies TCs by examination of the 850 relative vorticity field but then fixes the TC center to the nearest local MSLP minimum (Heming, 2017). The method's key advantage is that it gives a strong indication of the approximate center of the TC even for weak systems and does not depend on the ‘TC-Vitals’ information for tracking.

4.2. *Observed and predicted tracks (0000 and 1200 UTC)*

Track predictions obtained for the cyclone ‘Amphan’ from NCUM-G and NCUM-R based on various initial conditions (ICs) from 16-20 May, 2020 during 0000 and 1200 UTC are shown in Fig. 6. Though the cyclone track predictions from both NCUM model versions (global and regional) depict slight discrepancies with varying ICs compared with the IMD best track (black curve), most of the track forecasts indicate the cyclone landfall over West Bengal and Bangladesh regions. Compared with the IMD track, cyclone track prediction is more accurate and consistent in Day-1 (green) and Day-2 (purple) from NCUM-G and NCUM-R, which were initialized with 18-19 May, 2020 analysis, respectively. Track forecast based on 0000 and 1200 UTC of 16th May, 2020 in NCUM-G (0000 and 1200 UTC NCUM-R) indicates the

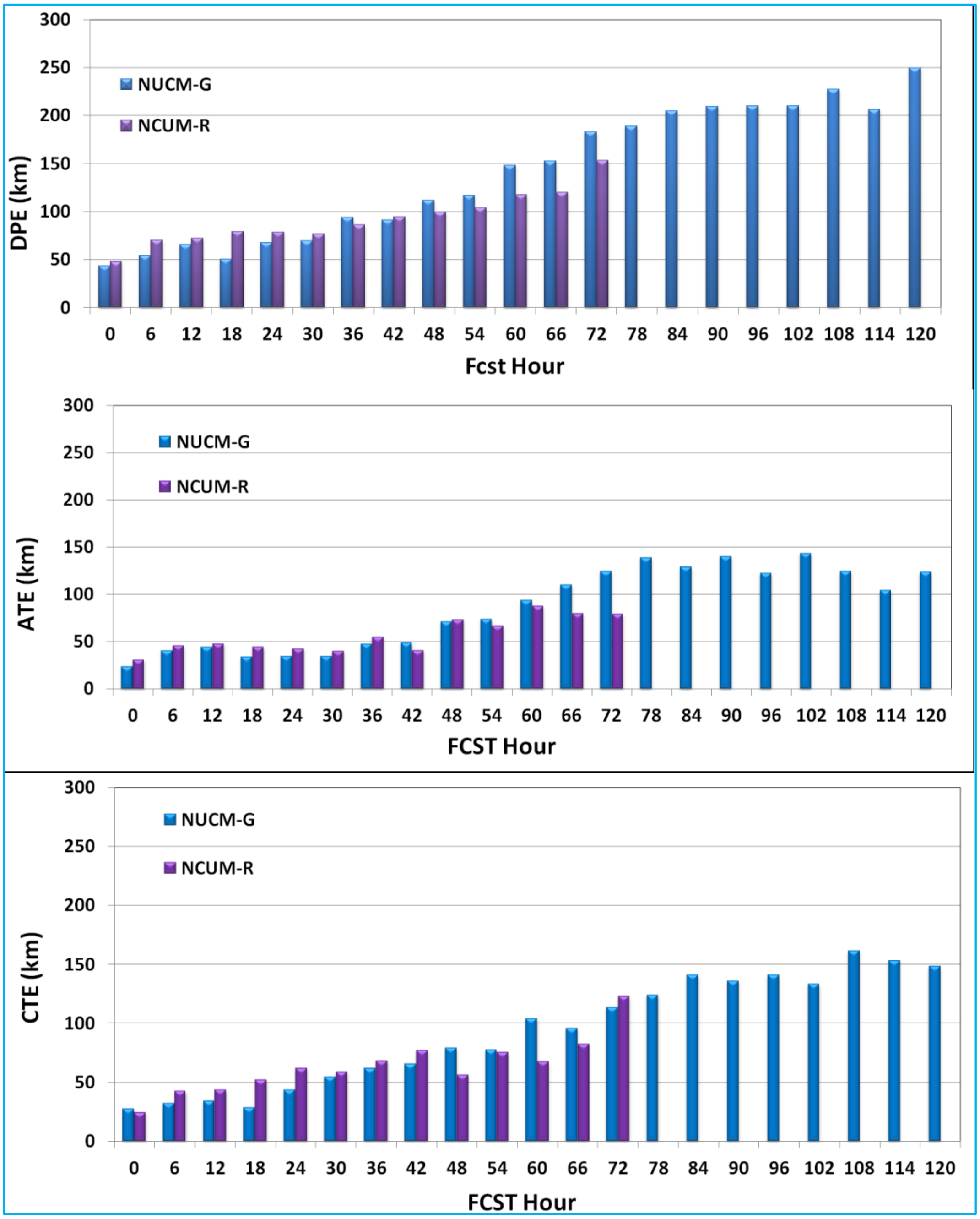

Fig. 7. Forecast tracks for cyclone Amphan based on NCUM-G and NCUM-R during 16-20 May, 2020

highest error,with the track being much to the east of the observed track. Similarly, the track forecast based on 17^{th} May also is shifted eastwards; however, with an improved track compared to the track predicted based on 16^{th} May.

4.3. *Forecast track errors*

The NCUM-G and NCUM-R tracks based on 0000 and 1200 UTC forecasts from 13-20 May, 2020 have been used in the verification. Table 4 summarizes the track errors at different lead times. The track error components of the direct position error (DPE), along track error (ATE) and cross track error (CTE), are shown in Fig. 7. The computation of DPE, ATE and CTE follows the method described in Heming (2017). It is noted that the early forecasts during 16^{th} and 17^{th} May, 2020 predicted the track much to the east of the observed track (Fig. 6), which is reflected in high CTE values at higher lead times.

TABLE 4

Forecast Track Errors for SCS Amphan from 13-21 May, 2020. NCUM-G, NEPS-G and NCUM-R track errors are based on 0000 UTC and 1200 UTC (numbers in the brackets indicate number of cases)

Forecast Hour	0	24	48	72	96	120
NUCM-G	43 (10)	68 (12)	112 (12)	183 (11)	210 (10)	250 (8)
NCUM-R	48 (11)	78 (12)	99 (12)	153 (11)	-	-

TABLE 5

Forecast track errors before the naming of the cyclone (13-15 May, 2020) and after the naming of cyclone (16-21 May, 2020)

Forecast Hour	0	12	24	36	48	60	72	84	96	108	120
Forecasts based on 13-21 May, 2020											
NCUM-G	43	65	68	94	112	148	183	205	210	227	250
NCUM-R	48	72	78	86	99	118	153	-	-	-	-
Forecasts based on 13-15 May, 2020											
NCUM-G		144	94	70	86	81	140	146	139	159	171
NCUM-R		80	63	59	93	103	138	-	-	-	-
Forecasts based on 16-21May, 2020											
NCUM-G	43	58	62	98	124	187	237	294	326	429	
NCUM-R	48	71	81	95	102	131	169	-	-	-	-

TABLE 6

Error in the forecast landfall time and position
(Forecast time – Observed time) [*-ve = early +ve = delay*]

IC	NCUM-G		NCUM-R	
	Time error (hr:min)	Position error (km)	Time-error (hr:min)	Position error (km)
0000 UTC 16052020	-11:00	263	-	-
1200 UTC 16052020	-07:30	200	-	-
0000 UTC 17052020	-04:00	105	-	-
1200 UTC 17052020	-03:30	200	-04:00	145
0000 UTC 18052020	01:00	143	-00:30	57
1200 UTC 18052020	-03:30	23	-00:30	26
0000 UTC 19052020	-02:00	37	0:00:	0
1200 UTC 19052020	-01:00	12	0:00:	12
0000 UTC 20052020	-00:30	8	1:30:	5

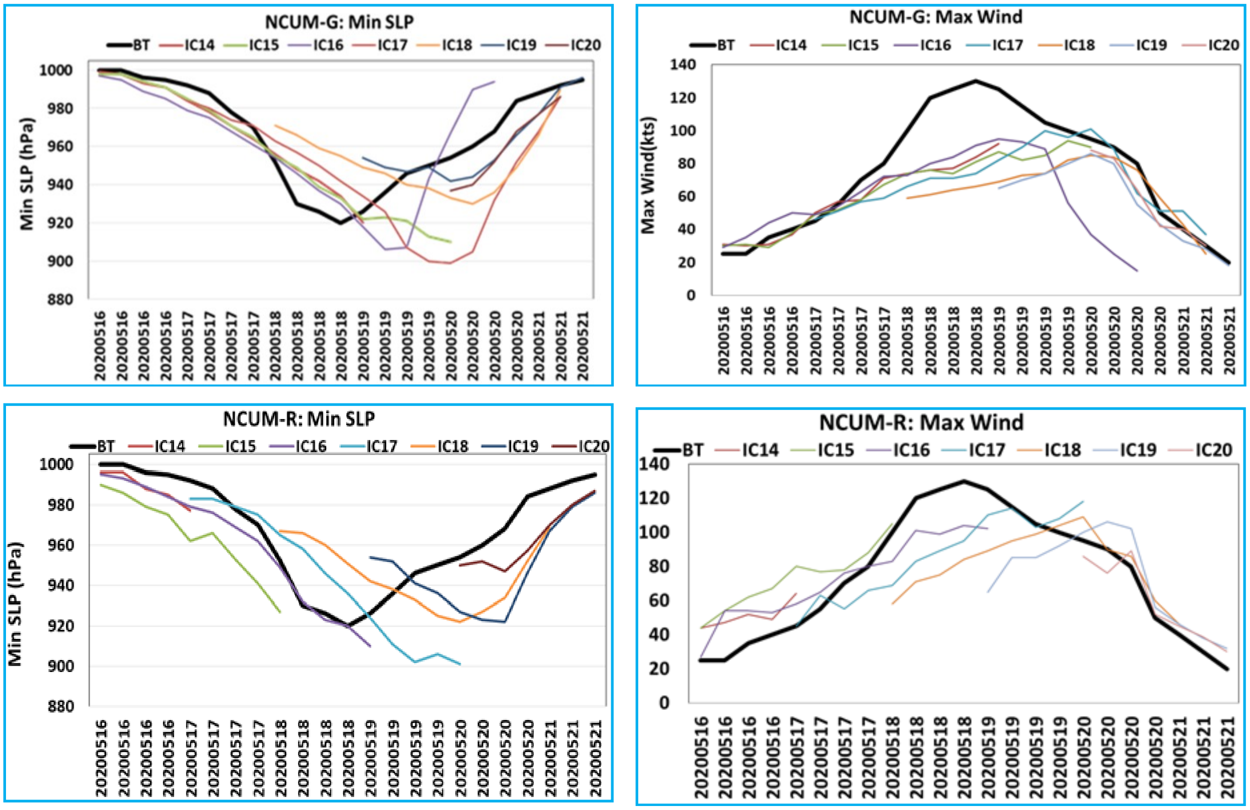

Fig. 8. Observed and forecast Min SLP (hPa) (left) and Max Wind (right) in the global model NCUM-G (top) and regional model NCUM-R (right) during 16-21 May, 2020

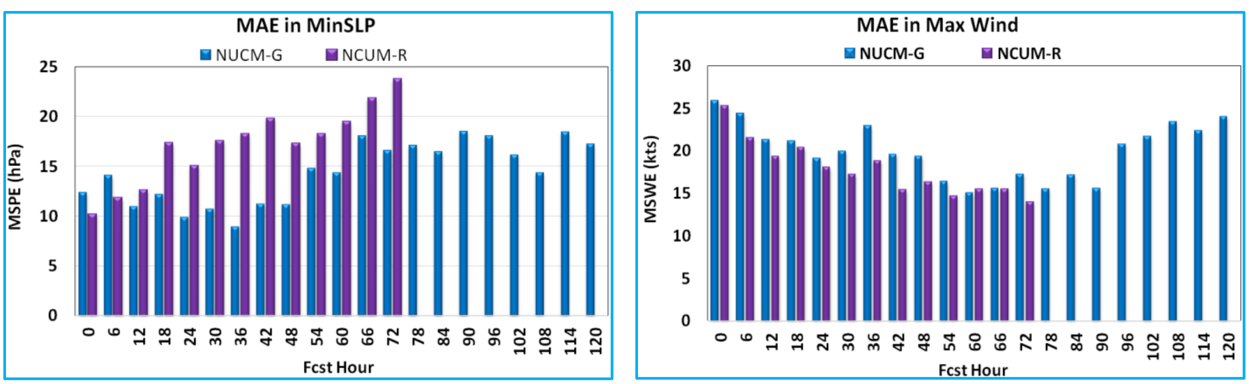

Fig. 9. Mean squared error in Min SLP (top) and Max wind (bottom) in the NCUM-G and NCUM-R forecasts of Super Cyclone 'Amphan' during 16-21 May, 2020

The mean initial position error is lowest in NCUM-G at 43 km. The 24 hr DPE ranges between 48-68 km, the 48 hr DPE ranges between 99-133 km and the 72 hr DPE ranges from 153-197 km. The DPE computed based on the forecasts for 13-15th May (Table 5) indicates lower values than the DPE values based on forecasts during 16-20 May, 2020. This possibility suggests higher DPE during and after the intensification of the cyclone.

4.4. *Forecast landfall position and time errors*

Forecast errors in landfall time and position from NCUM-G and NCUM-R are showed in Table 6. Forecasts made on 16th May, 2020 had relatively large errors both in landfall position (>200 km) and time of over 7-11 hours (early). Large position errors in forecasts with ICs before 0000 UTC on 18th May are consistent with large CTE

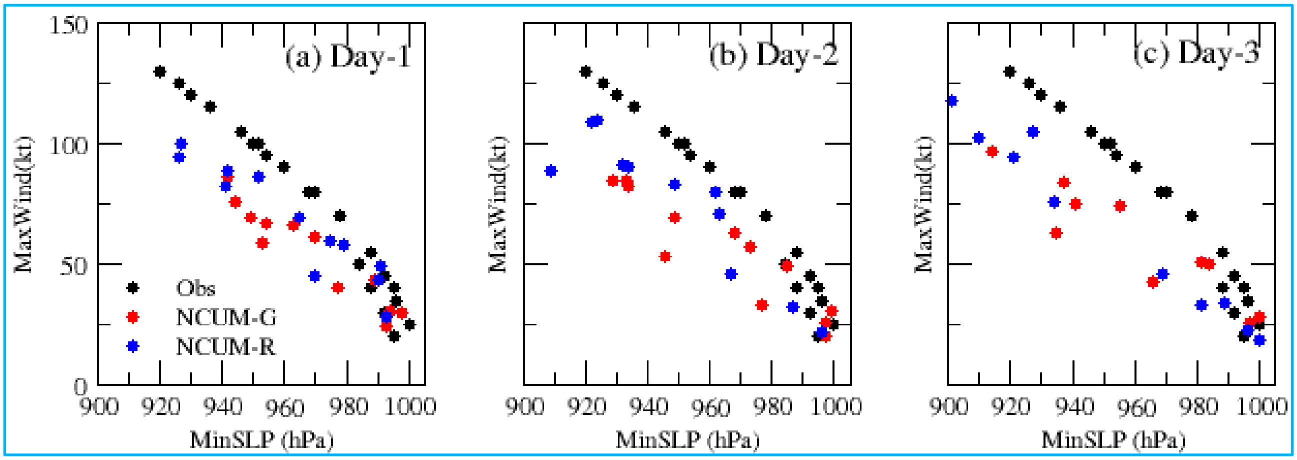

Figs. 10(a-c). Observed and forecast wind-pressure relationship for Super Cyclone 'Amphan' during 16-21 May, 2020

shown in Fig. 7. This is evident in the CTE magnitudes at 36-60 hour lead times. The time error has reduced to 1.3-7 hours (early) for forecasts based on 17th May, 2020 IC and the landfall position errors are also lower. Nevertheless, the forecasts made after 0000 UTC 18th May, 2020 have an extremely low error in both landfall position and time (Table 6). This is consistent with low ATE values at lead times of under 30 hours in Fig. 7. The forecasts from NCUM-R show the least error in space and time.

4.5. *Forecast intensity*

The minima in SLP and maxima in winds indicate the intensity of the cyclone. The observed and forecast Minimum SLP and Maximum Winds are shown in Fig. 8. Delayed peak intensity is evident in the forecasts. The NCUM-R predicted (66 hrs) Minimum SLP based on 16th May, 2020 initial condition is close to the observed intensity of 920 hPa on 18th May, 2020 at 1800 UTC. However, the forecasted Maximum Wind speed of 102 kt is much lower than the observed magnitude of 125 kt. It is evident from Fig. 8 that the model forecasts consistently indicated delayed intensification. The mean absolute error (MEA) in Minimum SLP and Maximum Wind is shown in Fig. 9. The highest SLP errors at 24, 48 and 72-hour forecasts are in NCUM-R. The lowest errors are evident in NCUM-G. The MEA in the Max Wind in NCUM-G and NCUM-R are very close, suggesting no significant advantage of high resolution in this case.

The bias can also be seen in forecast pressure-wind curves shown in Fig. 10. For every forecast, both the model predicted and observed Min SLP and Max 10-m winds are paired at a specified lead time. Black, filled dots indicate observed pressure-wind pairs, while red and blue filled dots indicate particular forecasts from NCUM-G and NCUM-R, respectively, at the specified lead time. The scatter points from observations and forecasts tend to overlay when the system is weak. With increasing intensity, the forecasts tend to show growing bias (lower Min SLP and lower Max Winds).

4.6. *Rapid Intensification (RI)*

The RI is defined as an increase of intensity of about 30 kt (15.4 ms^{-1}) in 24-h (IMD, 2015). As per the IMD official reports on 16th May, the system intensified from Depression (D) to Deep Depression (DD) and Cyclonic Storm (CS) on the same day. Moving nearly northwards, it further intensified into a Severe Cyclonic Storm (SCS) over southeast BoB in the morning of 17th May. It underwent rapid intensification (RI) during the next 24 hours and accordingly intensified into a Very Severe Cyclonic Storm (VSCS) by the afternoon of 17th May, Extremely Severe Cyclonic Storm (ESCS) in the early hours of 18th and into a SuCS around noon of 18th May, 2020. The forecasts show very strong intensification (Fig. 8) in both the global (NCUM-G) and regional (NCUM-R) model. However, the time of intensification is slightly different compared to the observations. The 24-hour change in the observed Max Wind associated with the cyclonic system is shown in Figs. 10(a&b). As reported, the cyclone underwent RI during 17-18 May, 2020, reflected in the obs (black) in Figs. 10(a-c). The 24-hour change in the reported Max wind remains higher than 30 kt from 0000 UTC on 17th May to 1800 UTC on 18th May. The NCUM-G forecasts, although they showed substantial intensification (Fig. 8), do not predict RI (NCUM-G Forecast based on 15th May comes closest to predicting the RI but misses by a narrow margin). The other forecasts rather show relatively gradual and rather late intensification.

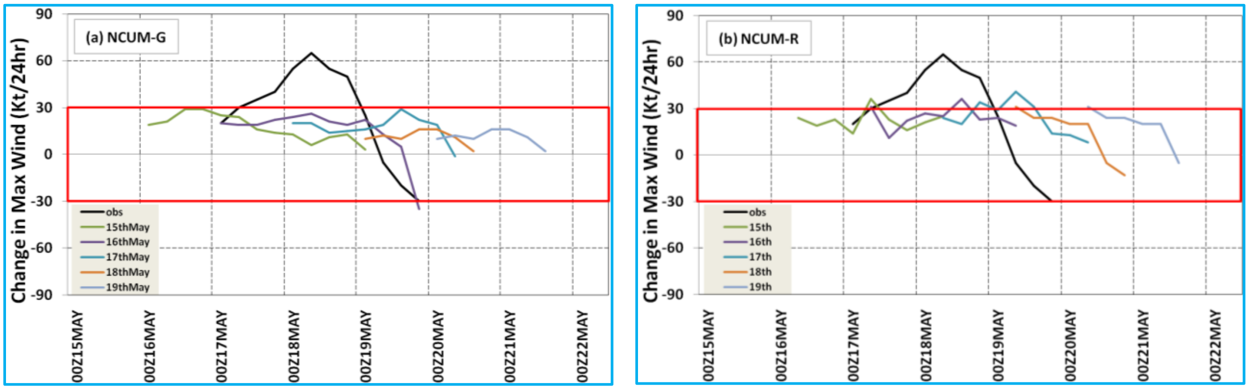

Fig. 11. Observed and forecast 24-hour change in the max wind speed associated with the SuCS 'Amphan' during 16-21 May, 2020

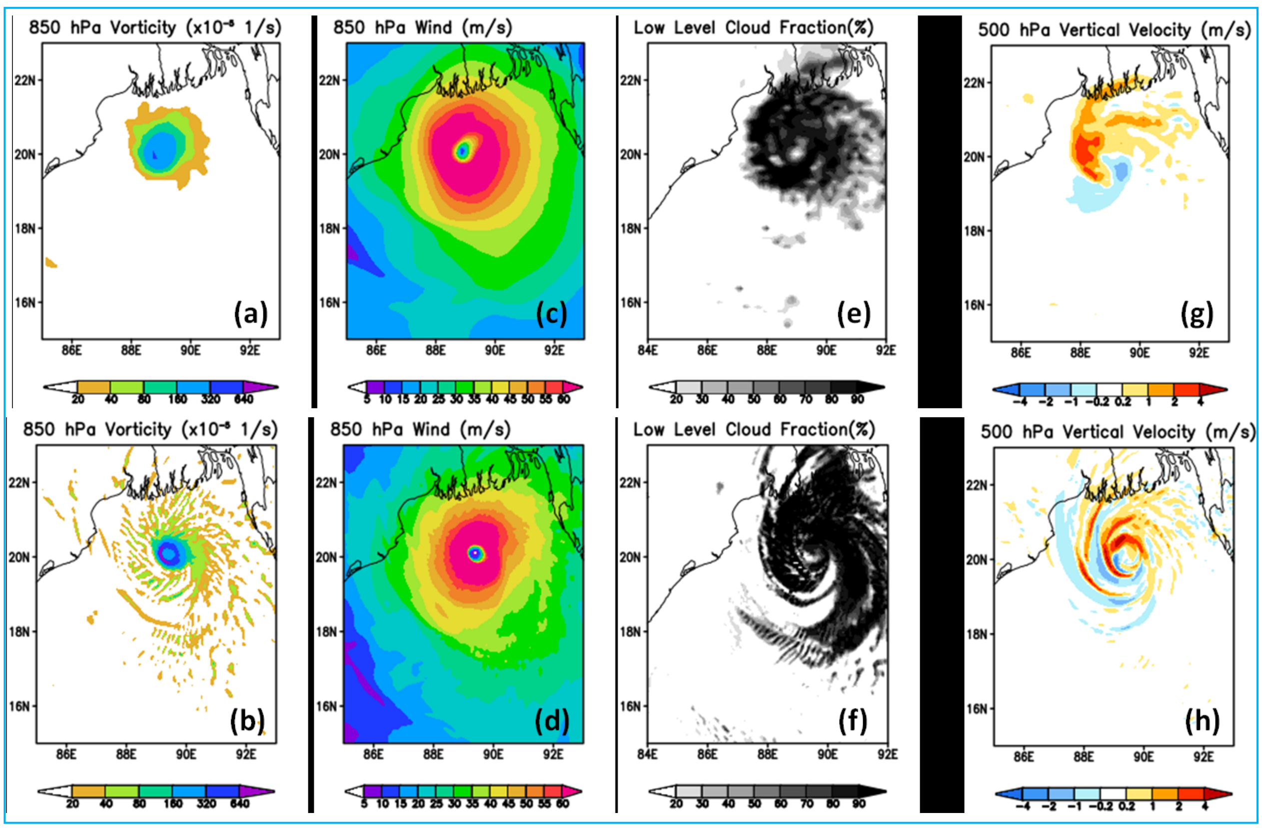

Figs. 12(a-h). A comparison of NCUM-G (top) and NCUM-R (bottom) forecast (Day-3) 850 hPa vorticity (a&b), 850 hPa wind speed (c&d), low level cloud fraction (e&f) and 500 hPa vertical velocity (g&h). The forecasts are valid at 0000 UTC 20th May, 2020

On the contrary, the NCUM-R forecasts show improved performance in predicting the RI. In the forecast based on 15th May, NCUM-R predicts RI at 0600 UTC on 17th May. Forecast based on 16th May also predicts RI at 1200 UTC on 18th May, much closer to the actual time of intensification, although late by few hours. Again the forecast based on 17th May, 2020 predicts RI at 0000, 0600 and 1200 UTC of 19th May, 2020. Thus, it can be concluded that the high resolution (4 km) forecasts based on NCUM-R show relatively improved performance compared to NCUM-G in predicting RI on 15th, 16th and 17th May, 2020.

5. Cyclone structure

Structure of TC in NCUM-G (12 km) and NCUM-R (4 km) forecasts are discussed here. An example of the structural differences arising from resolution differences

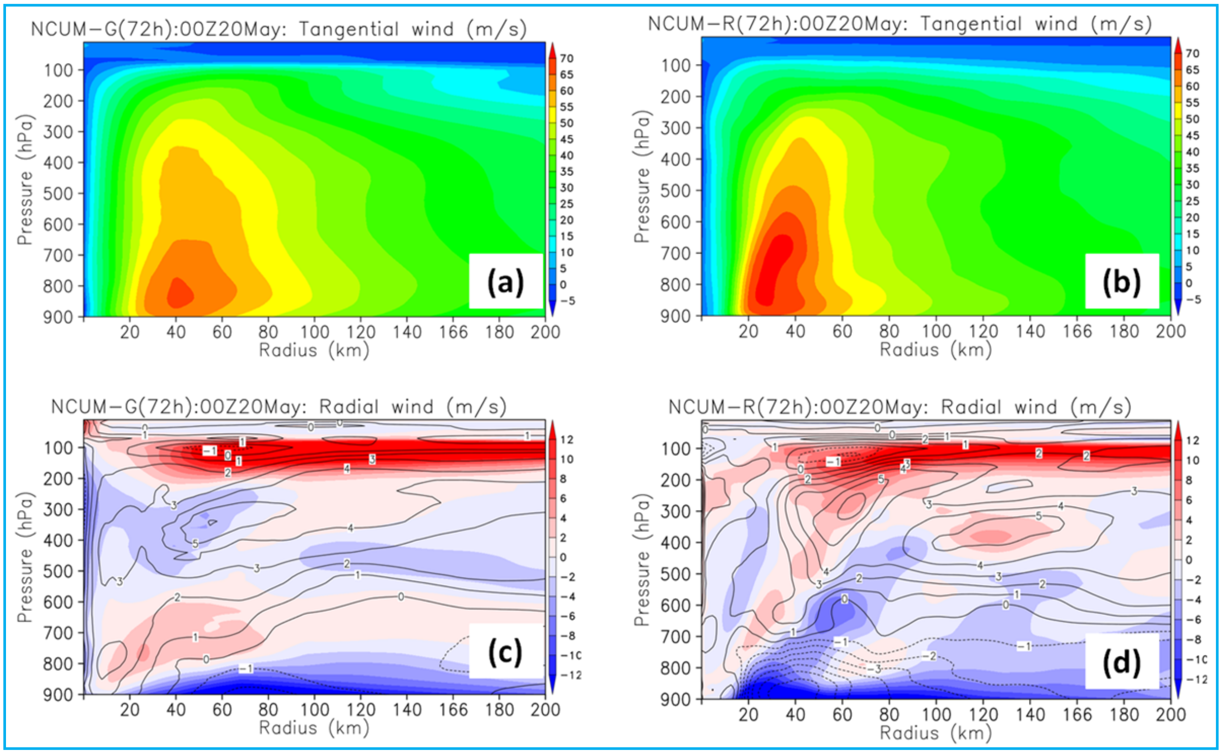

Figs. 13(a-d). Azimuthally averaged vertical cross-section of tangential (top) and radial wind (bottom) in NCUM-G (left) and NCUM-R (right) in the 72-hour forecast valid 0000 UTC 20th May, 2020. Positive (red) shaded region in bottom panels indicate radial inflow and negative (blue) shaded region indicate radial outflow. Contours show azimuthally averaged zonal wind

in the forecast of TC is shown in Figs. 12(a-h). The panels in the top row (Figs. a, c, e & g) correspond to NCUM-G and the panels in the bottom row correspond to NCUM-R. All the plots correspond to 72-hour forecast based on 17th May, 2020. In the high-resolution NCUM-R, the 850 hPa vorticity core of cyclone Amphan becomes much stronger and possesses a more horizontal structure [Fig. 12(b)] compared to the NCUM-G (12 km) forecast [Fig. 12(a)]. Similar results are evident for both 850-hPa horizontal wind [Figs. 12(c&d)] and low-level cloud fraction [Figs. 12(e&f)], with the 4 km model generating stronger winds with, much tighter storm core and a cloud free eye as well as spiral rain bands branching off the central dense overcast region at the core of the cyclone [Fig. 12(e&f)]. The 12-km NCUM-G grid shows a relatively weaker, broader cyclonic structure. Lastly, the higher resolution of the NCUM-R allows for more intense updrafts at the 500 hPa level, with a corresponding downdraft in the eye region [Figs. 12(a-h)]. Strength of vertical motion is associated with the spiral rain bands can be assessed from Low-Level Cloud Fraction. The unrefined forecast in NCUM-G shows a relatively larger, weaker peak in vertical motion with only one ascent band present around the storm core [Fig. 12(g)]. The high resolution forecast in NCUM-R shows stronger and multiple peaks of vertical motion [Fig. 12(h)].

[Figs. 13(a-d)] show a snapshot of the azimuthally averaged vertical cross-section of tangential (top) and radial wind (bottom) in NCUM-G (left) and NCUM-R (right) in the 72-hour forecast initialized with 0110 UTC 17th May, 2020 analysis. The storm's wind speed minimum defines the center of the cross-section. The structural differences resulting from the model grid resolution is seen in this figure. Both surface radial inflow (negative values) and upper-level outflow (positive values) are stronger in NCUM-R [Fig. 13(c)] when compared to NCUM-G [Fig. 13(d)], indicative of a much stronger circulation associated with the cyclone. The NCUM-G forecast [Fig. 13(c)] shows a more vertically diffuse inflow core, indicating that near-surface momentum may not be as concentrated in the model's lowest levels, thereby decreasing the efficiency of taking sensible and latent heat energy from the ocean surface. This is also shown in the tangential wind [Figs. 13(a&b)], which indicates a higher maximum wind location with NCUM-R. Besides, NCUM-R exhibits tangential wind structure similar to that of traditional, strong TCs (calm

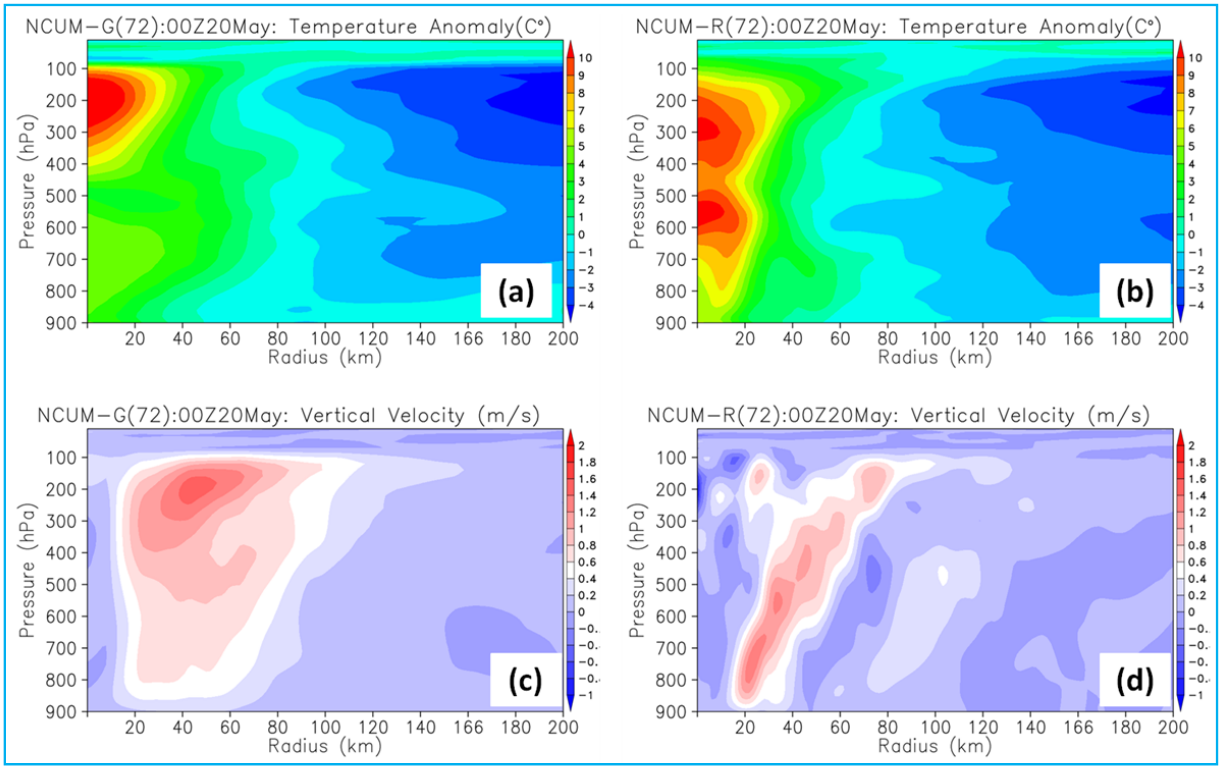

Figs. 14(a-d). Azimuthally averaged vertical cross-section of temperature anomaly (top) and vertical velocity (bottom) in NCUM-G (left) and NCUM-R (right) in the 72-hour forecast valid 0000 UTC 20th May, 2020. Positive shaded region in top panels indicate warm core region. Positive shaded regions in the bottom panels indicate region of strong upward motion

eye, sloped eyewall near-surface maximum wind). In contrast, the TC's structure in NCUM-G is less organized, with a radius of maximum wind approximately greater than that of NCUM-R.

[Figs. 14(a-d)] show a snapshot of the azimuthally averaged vertical cross-section of temperature anomaly (top) and vertical velocity (bottom) in NCUM-G (left) and NCUM-R (right) of 72-hour forecast initialized at 0000 UTC 17th May, 2020. The temperature anomaly [Figs. 14(a&b)] clearly shows the cyclone's warm core structure much more organized in NCUM-R. The vertical pressure velocity [Fig. 14(c&d)] also highlights the intensity differences between model runs. NCUM-R shows a deep, penetrating updraft core in the eyewall, whereas NCUM-G shows a much broader, weaker, more tilted updraft. Thus, the impact of high-resolution NCUM-R forecasts in improved representation of the cyclone intensity and structure is evident from the figures.

6. Summary

This study focused on comparative analysis of the recent SuCS 'Amphan' forecasts by assesses 4 km regional model NCUM-Rand 12 km resolution global model NCUM-G. Both the models are operationally being used at NCMRWF for NWP. The findings of this study can be summarized as follows.

(*i*) The space-time evolution of SuCS 'Amphan' in NCUM global and regional analyses is realistic even from the early stage of a well-marked low-pressure system. Further, during its intensification and its life-span as the intense cyclonic storm, the two analyses capture the system reasonably well. Similarly, the forecast track and intensity of the SuCS Amphan are well captured in the global and regional models accurately up to three days in advance and reasonably well up to five days.

(*ii*) Track error statistics show that the mean initial position errors in the global (43 km) and regional (48km) models are very close. However, the 24, 48 and 72-hour forecast position errors in global (NCUM-G) are 68, 112 and 183 km, respectively, which are higher than errors of 78, 99 and 153 km of NCUM-R. Forecast track errors based on earlier initial conditions (13-15 May, 2020) are higher than the errors based on the initial condition after the formation of D onwards (16-21 May, 2020).

(*iii*) Predicted landfall position (and time) errors are greater than 200 km (and about 3-11hours late) in forecasts based on the ICs before 0000 UTC of 17th May, 2020. This is subsequently reduced to less than 50 km (30 min to 3 hr late) in the forecasts after 0000 UTC 18th May, 2020. NCUM-R forecasts feature the least error in landfall position (0 to 26 km) and time (30 min late to 0130 min early).

(*iv*) Time delay in attaining the peak intensity is noticed in the forecasts compared to observations. The NCUM-R predicted Minimum SLP based on 16th May, 2020 is close to the observed intensity of 920 hPa on 18th May, 2020 at 1800 UTC. However, the maximum forecast wind is 102 kt is lower compared to the observed 125 kt. It is found that the model predicted intensity is more realistic when the system is weak. However, with the increase of the observed intensity, the forecasts tend to show growing biases.

(*v*) As per the IMD reports, SuCS Amphan underwent rapid intensification (RI) from 17-18 May, 2020. Both global (NCUM-G) and regional (NCUM-R) models indicate strong intensification, although not at the right time compared to the observations. The NCUM-G forecasts, although they showed strong intensification, do not predict RI (NCUM-G Forecast based on 15th May is closest in predicting the RI but misses by a narrow margin). NCUM-R forecast based on 15th (& 16th) of May predicted RI at 0600 UTC on 17th May (& 1200 UTC on 18th May). The RI predicted by NCUM-R at 1200 UTC on 18th May, is much closer to the reported timing, although late by few hours. Again the forecast based on 17th May, 2020 predicted RI at 0000, 0600 and 1200 UTC on 19th May, 2020.

(*vi*) Concerning track forecast, both NCUM-G and NCUM-R shows an impressive and significant reduction in errors. However, for predicted intensity forecasts both global and regional models feature strong and delayed intensification. It is found that accurate representation of intensity in the initial conditions still has scope for improvement.

(*vii*) An investigation of the structural differences in the TC forecast arising from resolution differences is further carried out. It is found that the high-resolution NCUM-R forecasts show the 850 hPa vorticity core (850 hPa wind, low-level cloud fraction, more intense updraughts at 500 hPa) of the cyclone Amphan, which is much stronger and possesses more horizontal structure with cloud free eye compared to the 12 km resolution NCUM-G.

(*viii*) Azimuthally averaged vertical cross-sections of tangential and radial wind forecasts from NCUM-G and NCUM-R are assessed for a deeper understanding of the structural differences resulting from the model grid resolution. Stronger surface radial inflow (and upper-level outflow) in NCUM-R is indicative of a much stronger circulation. NCUM-R exhibits a tangential wind structure similar to traditional, strong TCs (calm eye, sloped eyewall near-surface maximum wind). In contrast, the NCUM-G TC structure is less organized, with a radius of maximum wind greater than that of NCUM-R.

(*ix*) Vertical cross-section of temperature anomaly clearly shows that the cyclone's warm core structure's warm core structure is much more organized in NCUM-R. The cross-section of vertical pressure velocity field also highlights the intensity differences between model forecasts of NCUM-R and NCUM-G, where NCUM-R shows a deep and penetrating updraft core in the eyewall, which is missing in NCUM-G.

Acknowledgments

The first author thanks Dr. E. N. Rajagopal, former Head NCMRWF for providing the opportunity to compile and write this paper and for the encouragement and inspiration. The authors, thank the Cyclone Warning Division (CWD) of the India Meteorological Department (IMD), provide the best track data used in the verification of the model forecasts. The authors acknowledge Mike Fiorino, NOAA, USA for useful discussions and technical expertise for tropical cyclone analysis. The contents and views expressed in this research paper/article are the views of the authors and do not necessarily reflect the views of the organizations they belong to.

References

Ashrit, R. G., Gupta, M. Das and Bohra, A. K., 2006, "MM5 simulation of 1999 Orissa Super Cyclone : Impact of bogus vortex on track and intensity prediction", *MAUSAM*, **57**, 1, 129-134.

Balaji, M., Chakraborty, Arun and Mandal, M., 2018, "Changes in tropical Cyclone activity in north Indian Ocean during satellite era (1981-2014)", *Int. J. Climatol*., **38**, 6, 2819-2837, https://doi.org/10.1002/joc.5463.

Boutle, I., Eyre, J. and Lock, A., 2014, "Seamless stratocumulus simulation across the turbulent gray zone", *Mon. Wea. Rev*., **142**, 4, 1655-1668.

Bush, M., Allen, T., Bain, C., Boutle, I., Edwards, J., Finnenkoetter, A., Franklin, C. N., Hanley, K., Lean, H., Lock, A., Manners, J., Mittermaier, M. P., Morcrette, C., North, R., Petch, J., Short, C., Vosper, S., Walters, D. N., Webster, S., Weeks, M., Wilkinson, J., Wood, N. and Zerroukat, M., 2020, "The first Met Office Unified Model/JULES Regional Atmosphere and Land configuration, RAL1", *Geosci. Model Dev*., **13**. doi : 10.5194/gmd-2019-130.

Chourasia, M., Ashrit, R. G. and P. George, John, 2013, "Impact of cyclone bogusing and regional assimilation on tropical cyclone track and intensity predictions", *MAUSAM*, **64**, 1, 135-148.

Das, A. K., Rao, Y. R., Tallapragada, V., Zhang, Z., Bhowmik, S. R. and Sharma, A., 2015, "Evaluation of the Hurricane weather research and forecasting (HWRF) model for tropical cyclone forecasts over the North Indian Ocean (NIO)", *Nat. Hazards*, **75**, 1205-1221.

Dhanya, M., Gopalakrishnana, Deepak, Chandrasekar, A., Kumar Sing, Sanjeev and Prasad, V. S., 2016, "The impact of assimilating Megha Tropiques SAPHIR radiances in the simulation of tropical cyclones over Bay of Bengal using the WRF model", *International journal of Remote Sensing*, **37**, 13, 3086-3103.

Dutta, Devajyoti, Routray, A., Preveen Kumar, D., P. George, John and Singh, Vivek, 2019, "Simulation of a Heavy Rainfall Event during Southwest Monsoon using High-resolution NCUM-Modeling System : A Case Study", *Meteorology and Atmospheric Physics*, **131**, 1035-1054.

George J. P., Indira Rani, S., Jayakumar, A., Mohandas, Saji, Mallick, Swapan, Lodh, A., Rakhi, R., Sreevathsa, M. N. R. and Rajagopal, E. N., 2016, "NCUM Data Assimilation System", NMRF/TR/01/2016, p20. (https://www.ncmrwf.gov.in/NCUM-Report-Aug2018_final.pdf).

Hazelton, Andrew, Harris, Lucas and Lin, Shian-Jiann, 2018, "Evaluation of Tropical Cyclone Structure Forecasts in a High-Resolution Version of the Multiscale GFDL fvGFS Model", *Weather and Forecasting*, **33**, 10.1175/WAF-D-17-0140.1.IMD, 2015, "NWP report on cyclonic storms over the north indian ocean during 2014", IMD, January 2015.

Heming, J. and Goerss, J., 2010, "Track and Structure Forecasts of Tropical Cyclones", 2010, "World Scientific Series on Asia-Pacific Weather and Climate Global Perspectives on Tropical Cyclones", 287-323. https://doi.org/10.1142/9789814293488_0010.

Heming, J. T., 2017, "Tropical cyclone tracking and verification techniques for Met Office numerical weather prediction models", *Meteorol. Appl*., **24**, 1, 1-8.

Heming, J. T., Fernando Prates, Morris A. Bender, Rebecca Bowyer, John Cangialosi, Phillippe Caroff, Thomas Coleman, James D. Doyle, Anumeha Dube, Ghislain Faure, Jim Fraser, Brian C. Howell, Yohko Igarashi, Ron McTaggart-Cowan, M. Mohapatra, Jonathan R. Moskaitis, Jim Murtha, Rabi Rivett, M. Sharma, Chris J. Short, Amit A. Singh, Vijay Tallapragada, Helen A. Titley and Yi Xiao, 2019, "Review of Recent Progress in Tropical Cyclone Track Forecasting and Expression of Uncertainties", *Tropical Cyclone Research and Review*, **8**, 4, 181-218, ISSN 2225-6032. https://doi.org/10.1016/j.tcrr.2020.01.001.

Iyengar, G. R., Ashrit, Raghavendra, Ashish, Amit, Sharma, Kuldeep, Gupta, Munmun Das, Rajagopal, E. N. and Basu, Swati, 2014, "Improved prediction of cyclone Phailin (9-12 October 2013) with 4DVAR assimilation", *Current Science*, **107**, 6, 952-954.

Jayakumar, A., Steven, J. Abel, Andrew, G. Turner, Saji, Mohandas, Jisesh, Sethunadh, O'Sullivan, D., Mitra, A. K. and Rajagopal, E. N., 2019, "Performance of the NCMRWF convection-permitting model during contrasting monsoon phases of 2016 INCOMPASS field campaign", *Quarterly Journal of the Royal Meteorological Society*, **146**, 731, 2928-2948, doi:10.1002/qj.3689.

John, P. G., Indira Rani, S., Jayakumar, A., Mohandas, Saji, Mallick, Swapan, Rakhi, R., Sreevathsa, M. N. R. and Rajagopal, E. N., 2016, "NCUM Data Assimilation System", NMRF/TR/01/2016, March 2016.

Kumar, S., Jayakumar, A., Bushair, M. T., Buddhi Prakash, J., George, Gibies, Lodh, Abhishek, Indira Rani, S., Mohandas, Saji, George, John P. and Rajagopal, E. N., 2018b, "Implementation of New High Resolution NCUM Analysis-Forecast System in Mihir HPCS", NMRF/TR/01/2018, p17. (https://www.ncmrwf.gov.in/ NCUM-Report-Aug2018_final.pdf).

Kumar, S., Indira Rani, S., George, John P. and Rajagopal, E. N., 2018a, "Megha-tropiques SAPHIR radiances in a hybrid 4D-Var data assimilation system : Study of forecast impact", *Quarterly Journal of the Royal Meteorological Society*, doi: 10.1002/qj.3251.

Leroux, Kimberly Wood, Russell L. Elsberry, Esperanza O. Cayanan, Eric Hendricks, Matthew Kucas, Peter Otto, Robert Rogers, Buck Sampson and Zifeng Yu, 2018, "Recent Advances in Research and Forecasting of Tropical Cyclone Track, Intensity and Structure at Landfall", *Tropical Cyclone Research and Review*, **7**, 2, 85-105. ISSN 2225-6032, https://doi.org/10.6057/2018TCRR02.02.

Lock, A., Brown, A., Bush, M., Martin, G. and Smith, R., 2000, "A new boundary layer mixing scheme", Part I : Scheme description and single-column model tests, *Mon. Wea. Rev*., **128**, 9, 3187-3199.

Mandal, M., Mohanty, U. C., Potty, K. V. J. and Sarkar, A., 2003, "Impact of horizontal resolution on prediction of tropical cyclones over Bay of Bengal using a regional weather prediction model", *J. Earth Syst. Sci*., **112**, 1, 79-93. doi : 10.1007/BF02710045.

Mohanty, U. C., Osuri, K. K., Routray, A., Mohapatra, M. and Pattanayak, S., 2010, "Simulation of Bay of Bengal Tropical Cyclones with WRF Model : Impact of Initial and Boundary Conditions", *Marine Geodesy*, **33**, 4, 294-314.

Mohapatra, M., Nayak, D. P., Sharma, R. P. and Bandopadhyay, B. K., 2013, "Evaluation of official tropical cyclone track forecast over north Indian Ocean issued by India Meteorological Department", *J. Earth Syst. Sci*., **122**, 3, 589-601.

Nadimpalli, R., Krishna, K., Osuri, Mohanty, U. C., Anand, K. Das, Kumar, Ankur, Sil, S. and Niyogi, D., 2020, "Forecasting tropical cyclones in the Bay of Bengal using quasi-operational WRF and HWRF modeling systems : an assessment study", *Meteorol. Atmos. Phys*., **132**, 1-17. https://doi.org/10.1007/s00703-019-00669-6.

Osuri, K. K., Mohanty, U. C., Routray, A., Mohapatra, M. and Niyogi, D., 2013, "Real-Time Track Prediction of Tropical Cyclones over the North Indian Ocean Using the ARW Model", *Journal of Applied Meteorology and Climatology*, **52**, 2476-2492.

Osuri, K. K., Mohanty, U. C., Routray, A. and Niyogi, D., 2015, "Improved prediction of Bay of Bengal tropical cyclones through assimilation of Doppler weather radar observations", *Mon. Wea. Rev*., **143**, 4533-4560.

Osuri, K. K., Nadimpalli, R., Mohanty, U. C. and Niyogi, D., 2017, "Prediction of rapid intensification of tropical cyclone Phailin over the Bay of Bengal using the HWRF modelling system", *Q. J. R. Meteorol. Soc*., **143**, 678-690.

Pattanayak, S., Mohanty, U. C. and Gopalakrishnan, S. G., 2010, "Simulation of very severe cyclone Mala over Bay of Bengal with HWRF modeling system", *Nat. Hazards*, **52**, 1. doi: 10.1007/s11069-011-9863-z.

Prasad, V. S., Gupta, Anjari, Rajagopal, E. N. and Basu, Swati, 2013, "Impact of OSCAT surface wind data on T574L64 assimilation and forecasting system - A study involving tropical cyclone Thane", *Current Science*, **104**, 5, 627-632.

Rajagopal, E. N., Iyengar, G. R., George, John P., Gupta, Munmun Das, Mohandas, Saji, Siddharth, Renu, Gupta, Anjari, Chourasia, Manjusha, Prasad, V. S., Aditi, Sharma, Kuldeep and Ashish, Amit, 2012, "Implementation of the UM model based analysis-forecast system at NCMRWF", NMRF/TR/02/2012, p45. https://www.ncmrwf.gov.in/UM_OPS_VAR_Report.pdf.

Rawlins, F., Ballard, S. P., Bovis, K. J., A. Clayton, M., Li, D., Inverarity, G. W., Lorenc, A. C. and Payne, T. J., 2007, "The Met Office global four-dimensional variational data assimilation scheme", *Q. J. R. Met. Soc*., **133**, 347-362.

Routray, A., Singh, Vivek, George, John P., Mohandas, Saji and Rajagopal, E. N., 2017a, "Simulation of Tropical Cyclones over Bay of Bengal with NCMRWF Regional Unified Model", *Pure Appl. Geophys*., **174**, 1101-1119.

Routray, A., Singh, Vivek, Singh, Harvir, Dutta, Devajyoti, George, John P. and Rakhi, R., 2017b, "Evaluation of different versions of NCUM global model for simulation of track and intensity of tropical cyclones over Bay of Bengal", *Dynamics of Atmospheres and Oceans*, **78**, 71-88.

Saji, Mohandas and Ashrit, R., 2014, "Sensitivity of different convective parameterization schemes on tropical cyclone prediction using a mesoscale model", *Natural Hazards*, **73**, 2, 213-235.

Singh, O. P., Khan, Tariq Masood Ali and Rahman, Md. Sazedur, 2000, "Has the frequency of intense tropical cyclones increases in north Indian Ocean?", *Current Science*, **80**, 4, 575-580.

Srinivas, C. V., Venkatesan, R., Yesubabu, V., Nagaraju, C., Somayajai, K. M., Chellapandi, P and Baldev Raj, 2010, "Assimilation of conventional and satellite wind observations in a mesoscale atmospheric model for studying atmospheric dispersion", *Atmospheric Environment*, **44**, 24, 2846-2864.

Srinivas, C. V., Yesubabu, V., Prasad, K. B. R. R. H., Balasubramaniam, V. and Ramakrishna, S. S. V. S., 2012, "Numerical simulation of cyclonic storms FANOOS, NARGIS with assimilation of conventional and satellite observations using 3-DVAR", *Natural Hazards*, **63**, 867-889. https://doi.org/10.1007/s11069-012-0194-5.

Walters, D., Boutle, Ian, Brooks, M., Melvin, T., Stratton, R., Vosper, S., Wells, H., Williams, K., Wood, N., Allen, T., Bushell, A., Copsey, Dan, Earnshaw, P., Edwards, J., Gross, M., Hardiman, St., Harris, C., Heming, J., Klingaman, N., Levine, R., Manners, J., Martin, G., Milton, S., Mittermaier, M., Morcrette, C., Riddick, T., Roberts, M., Sanchez, C., Selwood, P., Stirling, A., Smith, C., Suri, D., Tennant, W., Vidale, P. L., Wilkinson, J., Willett, M., Woolnough, S. and Xavier, P., 2017, "The Met Office Unified Model Global Atmosphere 6.0/6.1 and JULES Global Land 6.0/6.1 configurations", *Geosci. Model Dev*., **10**, 1487-1520. doi:10.5194/gmd-10-1487-2017.

Wilson, Damian R., Bushell, Andrew C., M. Kerr-Munslow, Amanda, D. Price, Jeremy and Morcrette, Cyril J., 2008a, "A prognostic cloud fraction and condensation scheme, I : Scheme description", *Quarterly Journal of the Royal Meteorological Society*, **134**, 637. https://doi.org/10.1002/qj.333.

Wilson, Damian R., Bushell, Andrew C., M. Kerr-Munslow, Amanda, Price, Jeremy D., Morcrette, Cyril J. and Bodas-Salcedo, Alejandro, 2008b, "PC2 : A prognostic cloud fraction and condensation scheme. II : Climate model simulations", *Quarterly Journal of the Royal Meteorological Society*, **134**, 637. https://doi.org/10.1002/qj.332.